

A STRATEGY FOR MULTI-CAMERA ON-THE-JOB SELF-CALIBRATION

D. Brown, Melbourne, Florida

ABSTRACT

A photogrammetric configuration generated by multiple cameras can be amenable to effective self-calibration provided roll diversity is properly exploited. This finding has immediate and significant applications to measurements made in solar vacuum chambers by means of a new generation of equipment. In addition, it opens the door to photogrammetric operations in outer space that might otherwise be unfeasible.

1. INTRODUCTION

Over the past two decades the bundle adjustment with additional parameters has been used routinely in close-range photogrammetric nets to effect on-the-job self-calibration of the camera being employed. By now, the process has become standard — indeed, mandatory — practice for applications requiring highest attainable accuracies. As is pointed out in Chapter 22 of the ASPRS Second Edition of Non-Topographic Photogrammetry, several criteria must be met for self-calibration to be effective. First, a single camera must be used to take a set of at least three photos of the object. Second, both the interior geometry of the camera and the points to be measured on the object must remain stable during the period required for execution of the photography. Third, the photogrammetric network must have good geometric strength and must exercise photography of moderate to high convergence. Fourth, at least one photo must have a roll angle (i.e., angle about the camera axis) that is significantly different from the others (such roll diversity is indispensable). And, finally, a moderately large number (preferably in excess of 50) of well-distributed points should be triangulated in order to provide the level of redundancy necessary for an acceptable result. When all of these conditions are properly met, a complete and satisfactory calibration of the camera can be accomplished as an integral part of the triangulation without the need for control of any kind.

2. PHOTOGRAMMETRY IN SOLAR VACUUM TEST CHAMBERS

In one longstanding and important application of close-range photogrammetry the first of the above conditions for self-calibration cannot ordinarily be met. We refer to measurements of objects undergoing testing in solar vacuum chambers. Here, the camera, housed in its own vacuum-tight enclosure or canister, must operate under remote control within the confines of the chamber. Because it is impractical to move such a canisterized camera from one location to another, it is necessary to employ several individual canisterized cameras to generate an appropriate network. In the late 1960's Geodetic Services Inc. or GSI (then a division of DBA Systems, Inc.) developed a specialized photogrammetric system expressly designed for application in solar vacuum chambers. It consists of three remotely controlled, automatic plate changing cameras housed in individual canisters along with synchronized flash units. Major elements of the system are shown in Figure 1 (see Brown (1980) and Kenefick (1971) for details). Over the course of nearly 20 years this cumbersome one-of-a-kind system has been used to support testing in virtually every solar vacuum chamber in North America and has even been employed in an ESTEC chamber in Europe.

Because the above system is not directly amenable to self-calibration, an alternative approach referred to as *in situ* calibration has been devised. This process typically proceeds as follows. After the three canisterized cameras have been mounted in their fixed operating positions relative to the targeted object and before the chamber is to be evacuated, the pressure in each canister is increased to one atmosphere above ambient. This serves to duplicate the relative pressures between canister and chamber to be expected following pump down. At this point, under stable, ambient conditions a fourth, manually operated camera is introduced into the chamber. This camera is used to take a set of at least six photos of the object in conformance with the aforementioned requirements for self-calibration. As this is being done, each of the canisterized cameras also exposes a plate. In the subsequent bundle adjustment, photos from all four cameras are reduced simultaneously (typically, a nine station net). However, those from the fourth camera are recognized as having a common set of parameters for calibration while those from the canisterized cameras are each assigned a separate set of parameters. Although observations from all cameras are reduced in a single simultaneous adjustment, what this process effectively does is to establish a precise control network by virtue of the triangulation accomplished by the one camera amenable to self-calibration.

The coordinates thus generated serve as absolute control for the individual in-place (*in situ*) calibration of each of the canisterized cameras. The resulting calibrations are assumed to hold perfectly in subsequent operations following evacuation of the chamber. Whatever practical weakness there is in the process lies in this assumption. To bolster the validity of the assumption, the optical window in each canister is fabricated from thick (25 mm) fused quartz, and the temperature and pressure within each canister is maintained within a narrow range.

When first introduced, the system just discussed produced rms accuracies of triangulation on the order of 1 part in 60,000 of the maximum diameter of the object photographed. In recent years with the advent of automatic mensuration on AutoSet (Brown, 1987), accuracies have been pushed toward 1 part in 150,000. Even so, this falls far short of meeting the most stringent of current requirements which call for accuracies in mensuration of space antennas of better than 1 part in 500,000. To satisfy such accuracies a new system is needed along with a new, more powerful approach to calibration.

3. TOWARDS A NEW GENERATION OF CANISTERIZED CAMERAS

GSI has such developments underway. Fine details of instrumentation are beyond the scope of the present paper, primary emphasis here being on the new strategy for on-the-job self-calibration. Still, to place matters in proper context some aspects of hardware should be outlined. Most workers in the field of close-range photogrammetry have some familiarity with the STARS Turnkey System for Industrial Photogrammetry developed by GSI. At this writing more than 20 STARS systems are in operation in the U.S., Europe and Japan. A general description of STARS and its applications is to be found in Fraser, Brown (1986).

The camera employed in STARS is the CRC-1, a micro-processor controlled, large format (23 x 23 cm), roll film camera incorporating a back-projected reseau platen (Brown, 1984). Coupled with AutoSet for measuring its film, the CRC-1 has been refined to the point where it reliably produces closures of triangulation of better than 1 μm (rms) at photo scale. This translates to proportional accuracies on the order of 1 part in 300,000 for a strong six photo net in which all points are observed on all photos. From this one can expect that accuracies of 1 part in 600,000 are theoretically attainable from a sufficiently strong 24 photo net. It would thus seem that the CRC-1 provides a

logical starting point for a new system for use in solar vacuum chambers. There is, however, a flaw in this supposition. It concerns practical problems with photographic depth of field as characterized by the diameter C of the so called circle of confusion.

An acceptable value of C may be as little as $50 \mu\text{m}$; this would apply to images in the range of 40 to $60 \mu\text{m}$ in diameter which are generally considered to be of optimum size for human setting on a monocomparator. However, for automatic electronic setting (as with AutoSet) images of considerably larger size (100 to $150 \mu\text{m}$) are acceptable and, here, a value of C moderately in excess of $100 \mu\text{m}$ can be tolerated. Even so, such a generous circle of confusion presents a serious problem for a large format camera like the CRC-1 when operated within the restricted confines of the typical solar vacuum chamber. This stems ultimately from the fact that most solar vacuum chambers are relatively small, ranging generally from 5 to 10 meters in diameter.

To appreciate the significance of this, consider the specific situation indicated in Figure 2 which depicts in cross section a parabolic antenna 3 meters in diameter being photographed by one of several symmetrically arranged cameras, assumed here to be 240 mm CRC-1's. Such an antenna is about the largest that could be reasonably accommodated within the beam of a 6 meter solar vacuum chamber. As indicated in the figure, the camera is located at a radial distance of 2.4m from the vertex of the antenna and at a height of 2.4m above. The near and far field limits of the photographic field are 2.10 and 4.22 m , respectively. Figure 3 shows the expected appearance of a CRC-1 photo having a roll angle of 45° for a sample of points on the surface of the antenna. It is clear that the large format of the CRC-1 is fully utilized, and that the average photographic scale is consequently as large as possible.

It remains to be seen whether the focus of the photograph is acceptably sharp, particularly at the extremities of the field. The standard formulas defining acceptable depth of field of a photograph are (see, for example, Cox 1974):

$$(1) \quad a = \frac{fu (f + CN)}{(f^2 + uCN)}$$

$$(2) \quad b = \frac{fu (f - CN)}{(f^2 - uCN)}$$

in which

a = near field limit of photographic field,
 b = far field limit of photographic field,
 C = diameter of circle of confusion,
 f = focal length of lens,
 N = relative aperture (f number) employed,
 u = distance focused on.

From these equations one can derive the results:

$$(3) \quad u = \frac{a(b-f) + b(a-f)}{a + b - 2f}$$

$$(4) \quad C = \frac{b - a}{a(b-f) + b(a-f)} \frac{f^2}{N}$$

The above formulas are based on strictly geometric considerations and do not take into account the effects of diffraction which increase with increasing N. Thus, in practice, stopping a lens down (i.e., making N large) to gain depth of field eventually becomes counterproductive. However, for N as great as 32 (some might argue 45) the effects of diffraction remain tolerable and equation (4) is sufficiently valid.

If as in Figure 1 we set a = 4220 mm, b = 2100 mm and adopt f = 240 mm and N = 32, we obtain from (4) the value C = 236 μm for the diameter of the circle of confusion at near and far field limits. This is unacceptably large and stopping down further to N = 45 to produce a C = 168 μm is still insufficient. On the other hand, if the CRC-1 were left in the same position and a 120 mm lens were used, the value of C would be reduced somewhat more than fourfold to a more than acceptable value of 56 μm for N = 32. However, in this case only about half of the available format of the CRC-1 would be used, and the advantage of scale associated with the large format would be severely compromised.

From analyses such as the foregoing we have concluded with some reluctance that the full format of the CRC-1 would be largely underutilized in most applications likely to occur in solar vacuum chambers less than 10 meters or so in diameter. This consideration is one of several that prompted the development at GSI of the recently introduced CRC-2, a medium format (12 x 12 cm) companion to the CRC-1.

The two cameras are pictured side by side in Figure 4. Because the format of the CRC-2 is just over half that of the CRC-1, one might conclude that the accuracy to be expected from the CRC-2 is only about half that of the CRC-1. However, this is not necessarily the case, for a major goal in the design of the CRC-2 is that the camera produce accuracies equivalent to those of the CRC-1. What this means, in effect, is that rms closures of triangulation from the CRC-2 must be close to $0.50 \mu\text{m}$, or about half those typically achieved with the CRC-1.

The ultimate limitation to accuracies from the CRC-1 is set by the physical stability of the camera throughout the range of orientations involved in its use. By virtue of its smaller size, the CRC-2 is designed to be considerably more rigid without becoming unduly heavy. The vacuum platen of the CRC-2 is several times flatter than that of the CRC-1 and is stable to better than $0.50 \mu\text{m}$ in all orientations. Although the number of reseau points in the CRC-2 platen is the same as in the CRC-1 (25 in all), the density in terms of reseau images per unit area is four times as great. This leads to more accurate corrections for film deformation.

To complement the development of the CRC-2, GSI has also undertaken in parallel the development of AutoSet II, a successor of AutoSet I. With AutoSet II bidirectional repeatability of setting is 0.10 to $0.20 \mu\text{m}$ (vs. 0.30 to $0.40 \mu\text{m}$ for AutoSet I), rms accuracy of setting is 0.25 to $0.30 \mu\text{m}$ (vs. 0.40 to $0.50 \mu\text{m}$), and average speed of mensuration is just under two points per second (vs. one point per second). Thus AutoSet II is nearly twice as fast and twice as accurate as AutoSet I.

As this is written, the prototype of the CRC-2 has been extensively tested, and rms closures slightly over $0.60 \mu\text{m}$ have been achieved on a routine basis with film measured on AutoSet I. Meanwhile, AutoSet II is undergoing final testing and will be turned over to operations within a few weeks. We anticipate that the small further improvement required to produce closures of $0.50 \mu\text{m}$ will be achieved in due course once AutoSet II has been put to the task.

4. CANISTERIZED CRC-2

The relatively small size of the CRC-2 greatly simplifies the task of designing and fabricating a suitable canister for remotely controlled operations in a solar vacuum chamber. The canister currently being designed is of a simple cylindrical configuration, some 50 cm long and about 38 cm in diameter. An

optically flat, 80 mm diameter, 25 mm thick fused quartz window is mounted in the detachable lid of the canister. It serves as the optical port for the camera. This small, and almost optically perfect window is embedded in a larger (240 mm outside diameter) annular window which serves as the port for a ring strobe surrounding the lens. An opaque divider between the two concentric windows prevents light from the strobe unit from reflecting into the lens.

As mounted in the canister, the camera engages a special mechanism designed to permit the camera to be rotated about its axis under remote control. As shall be seen presently, this roll capability is vital to a new strategy for on-the-job self-calibration of the multiple cameras comprising the system. The weight of the canister (with camera and strobe equipment included) is expected to be under 35 kg. This is less than one sixth the weight of a loaded canister from the old system shown in Figure 1. Accordingly, the new system is far easier to install and much more convenient to operate.

5. SIMULATION OF A NEW STRATEGY FOR SELF-CALIBRATION

Extensive computer simulations have been performed to ascertain how best to proceed to attain, if possible, a level of accuracy on the order of 1:500,000 from a configuration of canisterized CRC-2 cameras. During the course of this investigation it was found that effective on-the-job self-calibration of a multi-camera configuration could be accomplished if each camera were to generate a succession of exposures of the object of interest differing significantly in roll angle from one frame to another. To illustrate this in a concrete way we shall review a single example. Consider again the set-up in Figure 2 which depicts a single camera observing a 3m antenna. At this point we shall assume the camera to be one of six symmetrically arranged CRC-2's of 120 mm focal length. The full configuration is illustrated in Figure 5. As was found earlier, if these cameras are stopped down to $N = 32$, the maximum circle of confusion has a diameter of only 56 μm , and this assures attainment of critically sharp imagery.

Key results of three computer simulations are summarized in Table 1. In each simulation rms measuring accuracy is taken as 0.50 μm in compliance with the design goal of the CRC-2, and images of 330 targeted points evenly distributed over the antenna are assumed to be measured on each negative.

TABLE 1. Results of computer simulations.

| | *STANDARD ERRORS OF TRIANGULATION (mm) | | | CORRESPONDING PROPORTIONAL ERRORS | | | |
|---|--|------------|------------|-----------------------------------|--------------|--------------|---------|
| | σ_x | σ_y | σ_z | σ_x/D | σ_y/D | σ_z/D | |
| | | | | (D = 3.0 m) | | | |
| | | | | 1 PART IN | | | |
| CASE 1. 6 photo net (6 cameras, 1 exposure each, perfect a priori camera calibrations). | Min. | .0058 | .0060 | .0083 | 517,000 | 500,000 | 361,000 |
| | Max. | .0134 | .0134 | .0099 | 223,000 | 223,000 | 303,000 |
| | Av. | .0091 | .0091 | .0094 | 330,000 | 330,000 | 319,000 |
| CASE 2. 24 photo net (same as Case 1, except that 4 exposures at orthogonal roll angles are reduced for each camera). | Min. | .0029 | .0030 | .0044 | 1,030,000 | 1,000,000 | 682,000 |
| | Max. | .0069 | .0069 | .0050 | 435,000 | 435,000 | 600,000 |
| | Av. | .0047 | .0047 | .0048 | 638,000 | 638,000 | 625,000 |
| CASE 3. 24 photo net (same as Case 2, except that each camera is subjected to self-calibration). | Min. | .0030 | .0031 | .0044 | 1,000,000 | 968,000 | 682,000 |
| | Max. | .0070 | .0070 | .0051 | 429,000 | 429,000 | 588,000 |
| | Av. | .0048 | .0048 | .0049 | 625,000 | 625,000 | 612,000 |

*Based on free net adjustment.

The basic six photo net of Case 1 provides an initial point of reference. It shows that if all six cameras were somehow perfectly calibrated, average proportional accuracies of better than 1:300,000 could be attained. This suggests that desired accuracies of better than 1:500,000 would be within reach if four times as many photos were reduced. This could, of course be accomplished in principle if a configuration of 24 cameras were employed — a dubious proposition from a practical standpoint. On the other hand, the requisite number of photos could be obtained in a more practical way if four exposures were made in rapid succession from each camera. This entails the normally undemanding assumption that the object remain perfectly stable over the short interval (about 15 seconds) required for such a photographic operation. However, it also entails the more shaky assumption that errors in measurements of each target are independent in successive frames from a given camera. This is unlikely when the film coordinates of the targets remain nearly the same from frame to frame, for then residual systematic errors stemming from both camera and comparator can also be expected to remain constant for each target. A simple and practical solution to this difficulty lies in rotating each camera a significant amount about its axis between successive exposures. This helps to 'randomize' systematic errors thereby enhancing the practical effectiveness of redundancy produced by repeated exposures. Because the roll maneuver can be accomplished as the film is being transported, this would not lengthen the time required for the photographic operation.

The foregoing scenario is simulated in Case 2 of Table 1. Here, each camera is assumed to be rolled nominally 90° between successive exposures. As can be seen from Table 2, the result of quadrupling the number of exposures in this manner is essentially to double accuracies of triangulation. Average proportional errors are now better than 1:600,000 in all three coordinates. However, this result, it must be kept in mind, is based on the continuing assumption that all six cameras are perfectly calibrated.

In the final simulation (Case 3) the assumption of perfect calibration is dropped, and the process of self-calibration is initiated. For each of the six cameras this involves carrying as additional unknowns in the bundle adjustment a set of eight interior projective parameters, namely: x_p , y_p , c (elements of interior orientation); K_1 , K_2 , K_3 (coefficients of radial distortion); P_1 , P_2 (coefficients of decentering distortion). As can be seen in Table 1, the effect of carrying these 48 additional parameters is to produce a result almost identical to that of Case 2 with increases in standard errors amounting to only 2 to 3 percent. This suggests that the additional parameters must be strongly recovered in the reduction, and this is indeed the case. For each of the six cameras the values produced for x_p , y_p and c have standard errors of 0.7, 0.7 and 1.1 μm , respectively. Moreover, the recovered radial and decentering distortion functions have standard errors of well under one micrometer at the maximum measured radial distance.

A striking general aspect of the results in Table 1 is the two to one range of accuracies in both X and Y from maximum to minimum as compared with the relative stability of accuracies in Z. Fortunately, in the present application the Z coordinate, being more nearly normal to the surface of the antenna, is of appreciably greater practical importance than X or Y and, accordingly, should be favored in the design.

With AutoSet II the time required for the entire process of mensuration of the set of 24 photos (about 360 points per photo counting fiducials and reseaus) would be under three hours. By virtue of this, the extra effort imposed by resorting to hyper redundancy is not unduly burdensome.

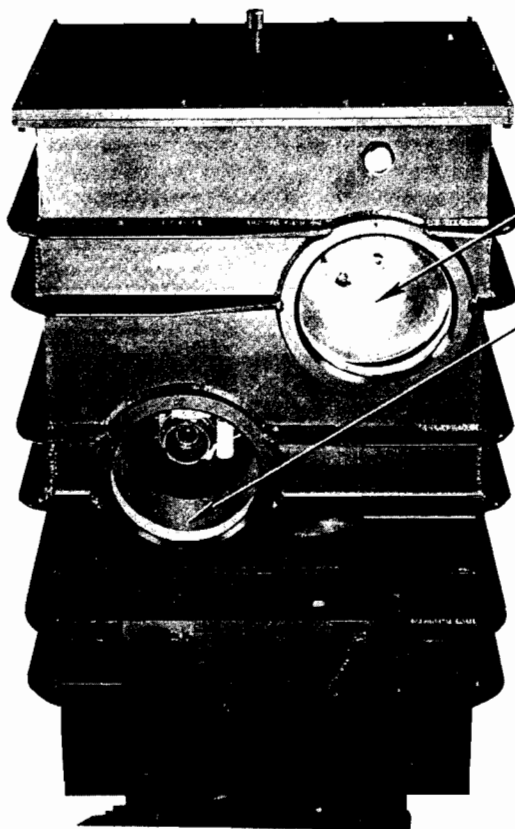
6. CONCLUSIONS

From the insight provided by the foregoing simulations we can pursue further developments with considerable confidence that accuracies of better than

1:500,000 can be obtained from photogrammetric operations conducted within solar vacuum chambers using the medium format CRC-2. A key consideration is that extra redundancy provided by repeated exposures can also lead to precise self-calibration provided each camera is rolled a significant degree between exposures. This frees the multi-camera configuration from being dependent on requirements of ultra-precise precalibration of cameras and accompanying assumptions of extended extreme stability. The new strategy for on-the-job self-calibration can also be beneficial in potential close-range photogrammetric operations on the Space Shuttle, for here the validity of terrestrial precalibration could be significantly compromised by weightlessness, not to mention stresses induced by launch into orbit.

7. REFERENCES

- BROWN, D.C., 1980. Application of Close-Range Photogrammetry to Measurements of Structures in Orbit. GSI Technical Report No. 80-012, Geodetic Services Inc., Florida, Vol. 1, 131 p.
- BROWN, D.C., 1984. A Large Format, Microprocessor Controlled Film Camera Optimized for Industrial Photogrammetry, Presented Paper, XV Congress of ISPRS, Commission V, Rio de Janiero, June, 29 p.
- BROWN, D.C., 1987. AutoSet, An Automated Monocomparator Optimized for Industrial Photogrammetry. Presented Paper, ISPRS International Conference and Workshop on Analytical Instrumentation, Phoenix, AZ, Nov., 16 p.
- COX, A., 1974. PHOTOGRAPHIC OPTICS, Fifteenth Revised Edition, Focal Press London and New York.
- KENEFICK, J.F., 1971. Ultra-Precise Analytics. Photogrammetric Engineering 37(11): 1167-1187.
- FRASER, C.S. and BROWN, D.C., 1986. Industrial Photogrammetry: New Developments and Recent Applications. Photogrammetric Record 12(68): 197-217.

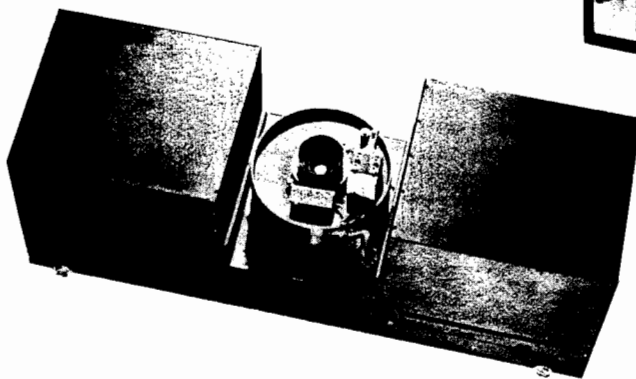
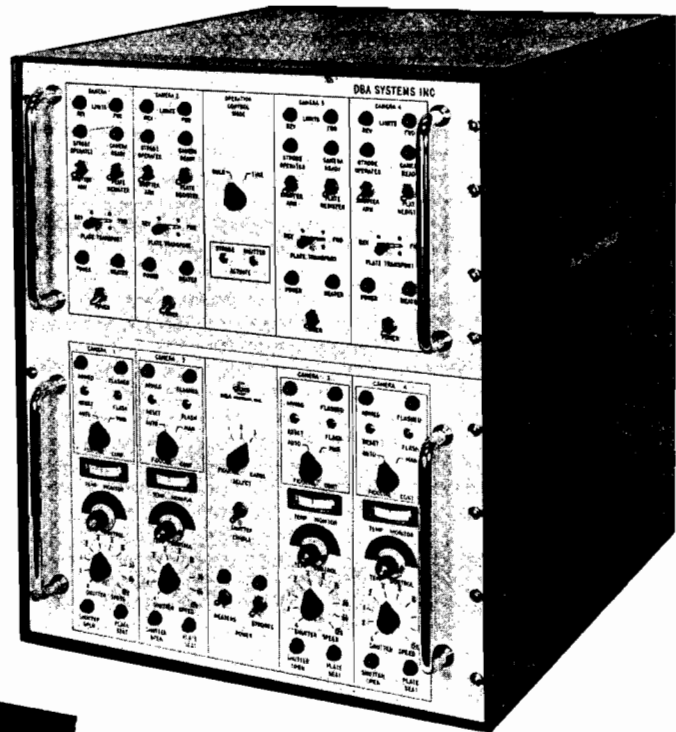


(a) Camera Canister
(withstands internal
pressures to 3
atmospheres)

Strobe Unit (1200 Watt Sec.)

Camera Port (25 mm thick, fused
quartz optical window)

(b) Control Unit



(c) Remotely Controlled, Automatic
Plate Changing Camera

Figure 1. Major components of system developed 20 years ago to permit photogrammetric mensuration of objects undergoing testing in solar vacuum chambers.

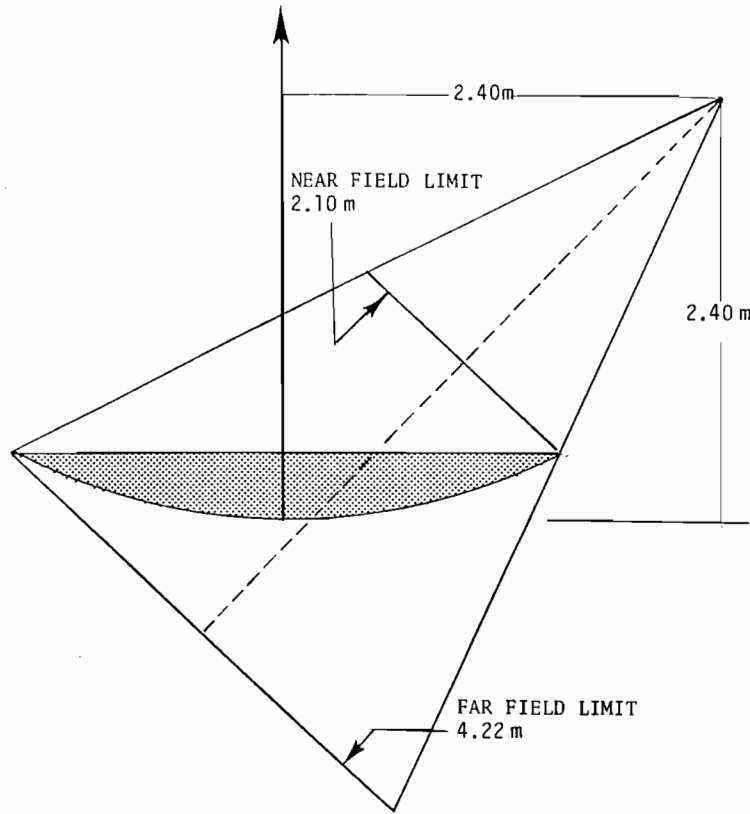


Figure 2. Typical convergent set-up for camera of 23 x 23 cm format and 240 mm focal length observing a 3 meter antenna in solar vacuum chamber.

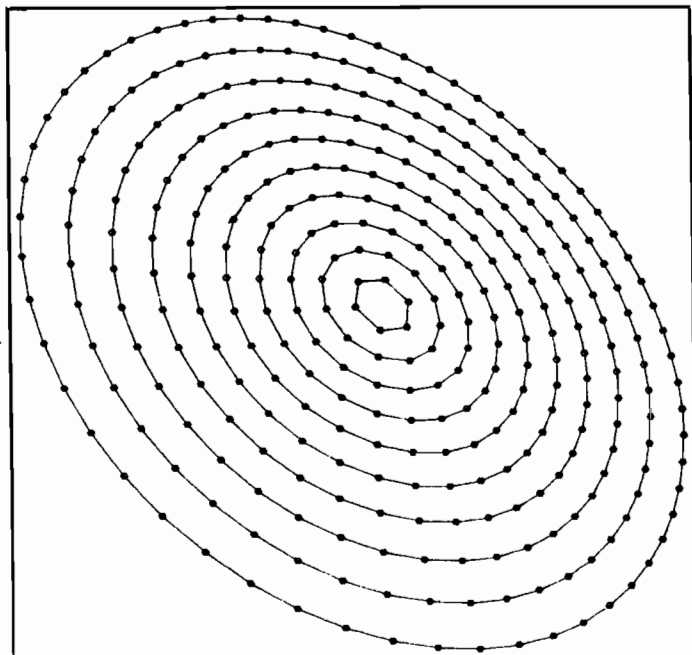


Figure 3. View of antenna as seen by camera for set of 330 targets. Roll angle is set at 45° in order to place semi-major axis of elliptical image of rim along diagonal of format.

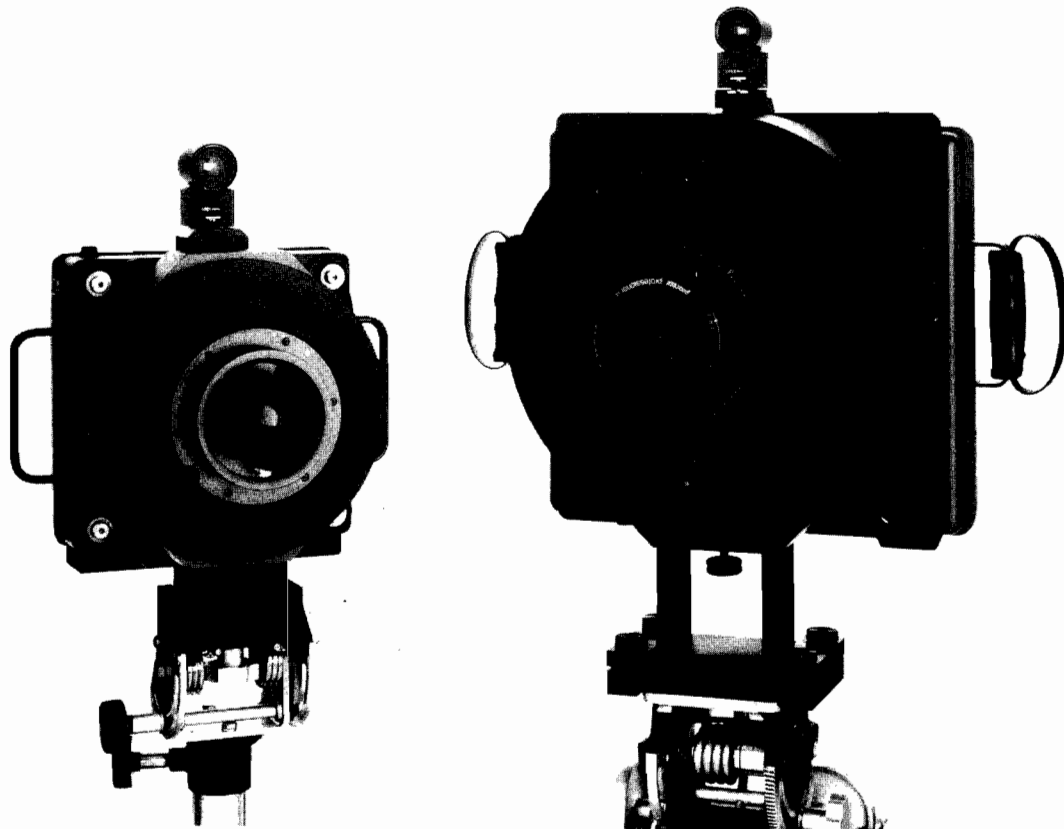


Figure 4. The 12 x 12 cm format CRC-2 camera alongside the 23 x 23 cm format CRC-1.

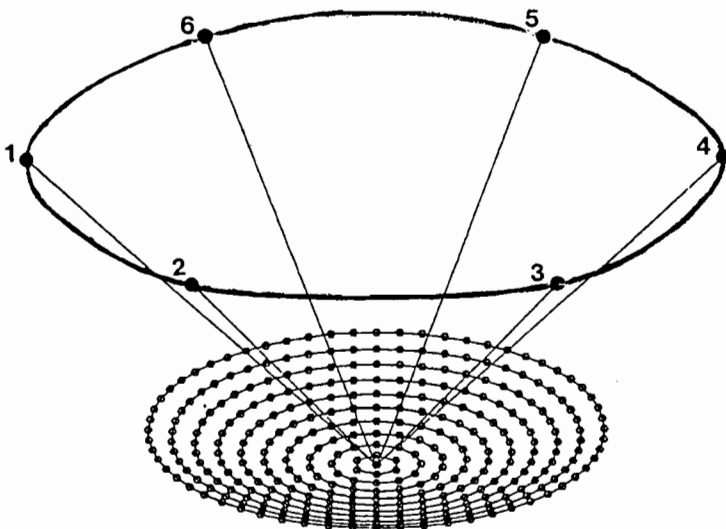


Figure 5. Geometry of 6 station set-up employed in computer simulations.

